

Regularization of time-varying covariance matrices using linear stochastic systems

Lipeng Ning

Abstract

This work focuses on modeling of time-varying covariance matrices using the state covariance of linear stochastic systems. Following concepts from optimal mass transport and the Schrödinger bridge problem (SBP), we investigate several covariance paths induced by different regularizations on the system matrices. Specifically, one of the proposed covariance path generalizes the geodesics based on the Fisher-Rao metric to the situation with stochastic input. Another type of covariance path is generated by linear system matrices with rotating eigenspace in the noiseless situation. The main contributions of this paper include the differential equations for these covariance paths and the closed-form expressions for scalar-valued covariance. We also compare these covariance paths using several examples.

Index Terms

Optimal control; linear stochastic system; Fisher-Rao metric; optimal mass transport;

I. INTRODUCTION

Consider a linear stochastic system

$$\dot{\mathbf{x}}_t = A_t \mathbf{x}_t + \sigma d\mathbf{w}_t, \quad (1)$$

where $A_t \in \mathbb{R}^{n \times n}$ and \mathbf{w}_t is a standard n -dimensional Wiener process. The corresponding state covariance $P_t := \mathcal{E}(\mathbf{x}_t \mathbf{x}_t')$ evolves according to

$$\dot{P}_t = A_t P_t + P_t A_t + \sigma^2 I, \quad (2)$$

This work was supported in part under grants R21MH115280 (PI: Ning), R01MH097979 (PI: Rathi), R01MH111917 (PI: Rathi), R01MH074794 (PI: Westin). L. Ning is with the Department of Psychiatry, Brigham and Women's Hospital, Harvard Medical School. Email: lning@bwh.harvard.edu

where I denotes the identity matrix. Given two positive definite matrices P_0, P_1 at $t = 0, 1$, respectively, we consider covariance paths that connect the two covariance given by the solution to the following problem

$$\min_{P_t, A_t} \left\{ \int_0^1 f(A_t) dt \mid (2) \text{ holds, and } P_0, P_1 \text{ specified} \right\}, \quad (3)$$

where $f(A_t)$ denotes a quadratic function of A_t which may depend on P_t . The optimal solutions to (3) could provide parametric models of covariance paths which are generalizations of shortest lines or geodesics. These paths could be applied to fit noisy measurements in order to understand the underlying system dynamics of stochastic processes.

In this paper, we investigate the solution to (3) corresponding to three objective functions, which have been explored in [1] using linear systems without stochastic input noise. Specifically, the first type of objective function quantifies the optimal mass transport cost between multivariate Gaussian distributions [2]–[5] when there is no stochastic noise. In the presence of noise, it has been recently extensively studied that the optimal solution becomes the covariance path induced by the Schrödinger Bridge Problem (SBP) [6] [7], [8]. The second objective function quantifies a type of weighted-mass-transport cost, which is also related to the Fisher-Rao metric from information geometry [9], [10]. The third family of objective function is given by the standard weighted-least-squares of the system matrices. The main contributions of this paper include the differential equation formulations of the optimal paths induced by the last two objective functions and the closed-form expressions in the special case of scalar-valued covariance.

The organization of this paper is as follows. In Section II we revisit covariance paths based on optimal mass transport and SBP. In Section III, we derive the covariance paths corresponding to a weighted-mass-transport cost function, which is equivalent to the Fisher-Rao metric in the noiseless situation. In Section IV, we investigate the covariance paths corresponding to the weighted-least-square functions, which includes the Fisher-Rao based covariance paths in a special case. In Section V, we compare these covariance paths using several examples. Section VI concludes the paper with discussions.

For notations, $\mathbb{S}^n, \mathbb{S}_+^n, \mathbb{S}_{++}^n$ denote the sets of symmetric, positive semidefinite, and positive definite matrices of size $n \times n$, respectively. Small boldface letters, e.g. \mathbf{x}, \mathbf{v} , represent column vectors. Capital letters, e.g. P, A , denote matrices. Regular small letters, e.g. w, h are for scalars or scalar-valued functions.

II. MASS-TRANSPORT BASED COVARIANCE PATHS

Consider $\mathbf{u}_t = A_t \mathbf{x}_t$ as the control input that steers the state covariance matrices according to (2). Define

$$f_{P_t}^{\text{omt}}(A_t) = \mathcal{E}(\|\mathbf{u}_t\|_2^2) = \text{tr}(A_t P_t A_t').$$

Then the minimum work needed to steer the covariance matrix from P_0 to P_1 is equal to

$$\min_{P_t, A_t} \left\{ \int_0^1 \text{tr}(A_t P_t A_t') dt \mid \dot{P}_t = A_t P_t + P_t A_t' + \sigma^2 I, \right. \\ \left. P_0, P_1 \text{ specified} \right\}. \quad (4)$$

If the noise component vanishes, i.e. $\sigma = 0$, then (4) gives the optimal mass transport distance [2]–[5] between two zero-mean Gaussian distributions with covariance matrices P_0 and P_1 , respectively. It is also related to the Bures distance between density matrices in quantum mechanics [11]–[13]. In the general situation when σ is non-zero, (4) can be viewed as the Schrödinger Bridge Problem (SBP) [6] between two zero-mean Gaussian probability density functions with covariance being P_0 and P_1 , respectively. The basic idea of SBP is to find a stochastic system whose probability law on the diffusion paths is most similar to that of a reference system measured by relative entropy and satisfies the initial and final marginal probability distributions. Its relations with stochastic optimal control and mass transport have been extensively studied recently [7], [8]. The more general situations when the reference model is a linear time-varying system with degenerate diffusions, i.e. noises that influence a subspace of the random states, have also recently been studied in [14], [15]. The following proposition presents the solution to (4).

Proposition 1. *Given $P_0, P_1 \in \mathbb{S}_{++}^n$ and a scalar σ . The unique set of solution to (4) is equal to*

$$A_t^{\text{omt}} = -\Pi_0 (I - \Pi_0 t)^{-1}, \quad (5)$$

$$P_t^{\text{omt}} = (I - \Pi_0 t) P_0 (I - \Pi_0 t) + \sigma^2 (I t - \Pi_0 t^2), \quad (6)$$

where

$$\Pi_0 = I - P_0^{-\frac{1}{2}} \left(\left(P_0^{\frac{1}{2}} P_1 P_0^{\frac{1}{2}} + \frac{1}{4} \sigma^4 I \right)^{\frac{1}{2}} - \frac{1}{2} \sigma^2 I \right) P_0^{-\frac{1}{2}}. \quad (7)$$

Proof. The optimization problem (4) is viewed as an optimal control problem with A_t being matrix-valued control input. A necessary condition for the optimal solution is that the derivative of the Hamiltonian

$$h_1(P_t, A_t, \Pi_t) = \text{tr}(A_t P_t A_t + \Pi_t (A_t P_t + P_t A_t' + \sigma^2 I))$$

with respect to A_t vanishes with the optimal control. This gives rise to

$$A_t P_t + \Pi_t P_t = 0.$$

Thus,

$$A_t = -\Pi_t. \quad (8)$$

Next, the optimal $\dot{\Pi}_t$ also needs to annihilate the derivative of $h_1(\cdot)$ with respect to P_t which leads to

$$\dot{\Pi}_t = -A_t' A_t - A_t' \Pi_t - \Pi_t A_t. \quad (9)$$

Substituting (8) to (2) and (9) to deduce that

$$\dot{P}_t = -\Pi_t P_t - P_t \Pi_t + \sigma^2 I, \quad (10)$$

$$\dot{\Pi}_t = \Pi_t^2. \quad (11)$$

Next, we show that all eigenvalues of the initial Π_0 must be smaller than one. For this purpose, we note that solutions for P_t and Π_t from (10) and (11) have the following form

$$P_t = (I - \Pi_0 t) P_0 (I - \Pi_0 t) + \sigma^2 (I t - \Pi_0 t^2), \quad (12)$$

$$\Pi_t = \Pi_0 (I - \Pi_0 t)^{-1}. \quad (13)$$

Assume that Π_0 has an eigenvalue $\lambda_0 > 1$, then $A_t = -\Pi_t$ becomes unbounded when t increases to $1/\lambda_0$. At the same time, P_t is singular at $t = 1/\lambda_0$ and becomes non positive semi-definite when $t > 1/\lambda_0$. Therefore, all eigenvalues of Π_0 are smaller than one.

Next, setting $t = 1$ in (12) and multiplying both sides by $P_0^{\frac{1}{2}}$ to obtain that

$$P_0^{\frac{1}{2}} P_1 P_0^{\frac{1}{2}} = \left(P_0^{\frac{1}{2}} (I - \Pi_0) P_0^{\frac{1}{2}} \right)^2 + \sigma^2 P_0^{\frac{1}{2}} (I - \Pi_0) P_0^{\frac{1}{2}}.$$

Therefore $P_0^{\frac{1}{2}}(I - \Pi_0)P_0^{\frac{1}{2}}$ has the same eigenvectors as $P_0^{\frac{1}{2}}P_1P_0^{\frac{1}{2}}$. If y is an eigenvalue of $P_0^{\frac{1}{2}}P_1P_0^{\frac{1}{2}}$, then the corresponding eigenvalue of $P_0^{\frac{1}{2}}(I - \Pi_0)P_0^{\frac{1}{2}}$, denoted by x , satisfies that $x^2 + \sigma^2x = y$. The two solutions are given by

$$x_{\pm} = -\frac{1}{2}\sigma^2 \pm (y + \frac{1}{4}\sigma^4)^{\frac{1}{2}}.$$

But x_- is negative which contradicts to that $I - \Pi_0$ is positive definite. Thus x_+ is the only feasible solution. Therefore,

$$P_0^{\frac{1}{2}}(I - \Pi_0)P_0^{\frac{1}{2}} = \left(P_0^{\frac{1}{2}}P_1P_0^{\frac{1}{2}} + \frac{1}{4}\sigma^4I \right)^{\frac{1}{2}} - \frac{1}{2}\sigma^2I,$$

which gives rise to the optimal solution in (7). Then, the proposition is proved. \square

We note that if Π_0 is singular, then A_t^{omt} is also singular for all $t \in [0, t]$, which implies free diffusion in the subspace spanned by the eigenvectors of Π_0 corresponding to zero eigenvalues. In the noiseless situation when $\sigma = 0$, then covariance path in (6) is equal to the geodesic induced by the Wasserstein-2 metric.

III. INFORMATION-GEOMETRY BASED COVARIANCE PATHS

The Fisher information metric has provided a well-defined distance measure between probability distributions. For zero-mean multivariate Gaussian distributions, the Fisher information metric can be expressed as a quadratic form of the covariance matrices, which is referred to as the Fisher-Rao metric [9], [10]. Specifically, let P be a positive definite covariance matrix and let Δ be a symmetric matrix denoting a tangent direction at P on the manifold of positive-definite matrices. Then the Fisher-Rao metric has the following form [10]

$$g_P(\Delta) = \text{tr}(P^{-1}\Delta P^{-1}\Delta).$$

The geodesic connecting P_0, P_1 induced by the Fisher-Rao metric is the optimal solution to

$$\min_{P_t, \dot{P}_t} \left\{ \int_0^1 \text{tr}(P^{-1}\dot{P}_t P^{-1}\dot{P}_t) dt \mid P_0, P_1 \text{ specified} \right\}. \quad (14)$$

The optimal solution has the following well-known expression [16]

$$P_t = P_0^{\frac{1}{2}}(P_0^{-\frac{1}{2}}P_1P_0^{-\frac{1}{2}})^t P_0^{\frac{1}{2}}. \quad (15)$$

In [1], we showed that this geodesic is also the optimal solution to an optimization problem in the form of (3) in the situation when the noise component $\sigma = 0$. Specifically, we denote

$$f_{P_t}^{\text{info}}(A_t) = \mathcal{E}(\|\mathbf{u}_t\|_{P_t^{-1}}^2) = \mathcal{E}(\mathbf{u}_t' P_t^{-1} \mathbf{u}_t) = \text{tr}(P_t^{-1} A_t P_t A_t').$$

Then, (15) is also the optimal solution to

$$\min_{P_t, A_t} \left\{ \int_0^1 f_{P_t}^{\text{info}}(A_t) dt \mid \dot{P}_t = A_t P_t + P_t A_t', P_0, P_1 \text{ specified} \right\}, \quad (16)$$

with the optimal system matrix given by the constant matrix

$$A = \frac{1}{2} P_0^{\frac{1}{2}} \log(P_0^{-\frac{1}{2}} P_1 P_0^{-\frac{1}{2}}) P_0^{-\frac{1}{2}}.$$

Note that the optimization problem (16) provides an interesting weighted-mass-transport view of the Fisher-Rao metric.

Following (3), we consider the optimization problem in below:

$$\min_{P_t, A_t} \left\{ \int_0^1 \text{tr}(P_t^{-1} A_t P_t A_t') dt \mid \dot{P}_t = A_t P_t + P_t A_t' + \sigma^2 I, \right. \\ \left. P_0, P_1 \text{ specified} \right\}. \quad (17)$$

A. On the optimal paths

Using variational analysis, we obtain the following proposition on the optimal solution to (17).

Proposition 2. *Given $P_0, P_1 \in \mathbb{S}_{++}^n$ and a scalar σ . If there exists a path that satisfies the following differential equation*

$$\dot{P}_t = -2P_t \Pi_t P_t + \sigma^2 I, \quad (18)$$

$$\dot{\Pi}_t = 2\Pi_t P_t \Pi_t, \quad (19)$$

with P_t being equal to P_0 and P_1 at $t = 0$ and 1 , respectively, then P_t is an optimal solution to (17). The corresponding A_t is equal to

$$A_t = -P_t \Pi_t. \quad (20)$$

Moreover, the path P_t also satisfies the following differential equation

$$\ddot{P}_t - \dot{P}_t P_t^{-1} \dot{P}_t + \sigma^4 P_t^{-1} = 0. \quad (21)$$

Proof. Following the same method as in the proof of Proposition (1), we will derive the solution to the optimal control problem (17) using the following Hamiltonian

$$h_2(P_t, A_t, \Pi_t) = \text{tr} \left(P_t^{-1} A_t P_t A_t' + \Pi_t (A_t P_t + P_t A_t' + \sigma^2 I) \right).$$

It is necessary that $\dot{\Pi}_t$ annihilates the partial derivative of $h_2(\cdot)$ with respect to P_t , which leads to

$$\dot{\Pi}_t = -A_t' P_t^{-1} A_t + P_t^{-1} A_t P_t A_t' P_t^{-1} - \Pi_t A_t - A_t' \Pi_t. \quad (22)$$

Moreover, setting the derivative of $h_2(\cdot)$ with respect to A_t to zero to obtain that

$$A_t = -P_t \Pi_t. \quad (23)$$

Then, (18) and (19) can be obtained by substituting (23) to (2) and (22), respectively. From (18), we obtain the following expression

$$\Pi_t = \frac{1}{2} (\sigma^2 P_t^{-2} - P_t^{-1} \dot{P}_t P_t^{-1}).$$

Next, taking the derivative of Π_t and setting it equal to (19) we obtain that

$$\begin{aligned} \dot{\Pi}_t &= \frac{1}{2} \left(\sigma^2 (-P_t^{-1} \dot{P}_t P_t^{-2} - P_t^{-2} \dot{P}_t P_t^{-1}) \right. \\ &\quad \left. + 2P_t^{-1} \dot{P}_t P_t^{-1} \dot{P}_t P_t^{-1} - P_t^{-1} \ddot{P}_t P_t^{-1} \right) \\ &= \frac{1}{2} (\sigma^2 P_t^{-2} - P_t^{-1} \dot{P}_t P_t^{-1}) P_t (\sigma^2 P_t^{-2} - P_t^{-1} \dot{P}_t P_t^{-1}). \end{aligned}$$

Then (21) can be obtained from the above equation after simplifications. Thus, the proof is complete. \square

In the noiseless situation when $\sigma = 0$, (21) becomes

$$\ddot{P}_t - \dot{P}_t P_t^{-1} \dot{P}_t = 0,$$

which is the geodesic equation induced by the Fisher-Rao metric [16], [17]. In this case, the

closed-form expression of P_t is given by (15). The closed-form expression of the optimal solution to (17) is currently unknown to the author except for the scalar-valued cases given in below.

B. The scalar case

Consider a scalar-valued covariance path p_t that is expressed by one of the following equations:

$$p_t = p_0 + \sigma^2 t, \quad (24)$$

$$p_t = ae^{bt} - \frac{\sigma^4}{4ab^2} e^{-bt}, \quad (25)$$

$$p_t = \frac{\sigma^2}{\omega} \cos(\omega t + \theta), \quad (26)$$

$$\text{with } 0 < \omega < \pi, -\frac{\pi}{2} < \theta < \frac{\pi}{2}.$$

It is straightforward to verify that all the above expressions satisfy that

$$p_t \ddot{p}_t - (\dot{p}_t)^2 + \sigma^4 = 0,$$

which is a scalar-version of (21). Clearly, (24) corresponds to a covariance path purely driven by the input noise. For the covariance path in (26), the constraint $0 < \omega < \pi$ is to ensure that P_t does not have negative values on $t \in [0, 1]$. Moreover, the constraint $-\frac{\pi}{2} < \theta < \frac{\pi}{2}$ guarantees that p_0 is positive. The following proposition shows that (25) and (26) connect covariance that satisfy different boundary conditions.

Proposition 3. *Given three positive scalars p_0, p_1 and σ . If $|p_1 - p_0| > \sigma^2$, then exists a unique solution to (17) which has the form of (25). If $|p_1 - p_0| < \sigma^2$, then there exists a unique solution to (17) which has the form of (26).*

Proof. Since the paths in (25) and (26) both satisfy the (21). We will prove that if $|p_0 - p_1| > \sigma^2$, then there exists a unique pair of parameters a, b such that p_t from (25) is equal to p_0 and p_1 at $t = 0, 1$, respectively and there exists no path of the form (26) that satisfies the boundary conditions. If $|p_1 - p_0| < \sigma^2$ then there exists a unique path of the form (26) and there exists no path of the form (25) that satisfies the boundary conditions.

To prove the first statement, we set p_t in (25) to p_0 and p_1 at $t = 0, 1$, respectively, to obtain

that

$$\begin{aligned} p_0 &= a - \frac{\sigma^4}{4ab^2}, \\ p_1 &= ae^b - \frac{\sigma^4}{4ab^2}e^{-b}. \end{aligned} \quad (27)$$

Then, we can derive the following

$$a = \frac{p_1 - p_0e^{-b}}{e^b - e^{-b}}.$$

Next, substituting the above expression into (27) then multiplying both sides by $4(p_1 - p_0e^{-b})b^2$ to obtain that

$$4(p_1 - p_0e^{-b})(p_1 - p_0e^b)b^2 - \sigma^4(e^b - e^{-b})^2 = 0. \quad (28)$$

The above equation has a trivial solution at $b = 0$. Moreover, if b is a solution to (28) so is $-b$. For a non-zero b that satisfies (28), the coefficient of the second term of p_t is equal to

$$-\frac{\sigma^4}{4ab^2} = \frac{p_1 - p_0e^b}{e^{-b} - e^b}.$$

Therefore, (25) is equivalent to

$$p_t = \frac{p_1 - p_0e^{-b}}{e^b - e^{-b}}e^{bt} + \frac{p_1 - p_0e^b}{e^{-b} - e^b}e^{-bt}.$$

Thus, switching b to $-b$ does not change the covariance path in (25). Therefore, we only consider positive solutions to (28). To this end, we denote the left hand side of (28) by $\phi(b)$. It is straightforward to derive that

$$\begin{aligned} \frac{d\phi(b)}{db} \Big|_{b=0} &= 0, \\ \frac{d^2\phi(b)}{db^2} \Big|_{b=0} &= 8((p_1 - p_0)^2 - \sigma^4). \end{aligned}$$

Moreover,

$$\frac{d^3\phi(b)}{db^3} = -4p_0p_1(e^b - e^{-b})(b^2 + 6b + 6) - 8\sigma^4(e^{2b} - e^{-2b})$$

which is negative for all $b > 0$. Therefore, if $(p_1 - p_0)^2 - \sigma^4 > 0$, then the function $\phi(b)$ is convex and positive near $b = 0$. But $\phi(b) < 0$ as $b \rightarrow \infty$. Because its second order derivative $\frac{d^2\phi(b)}{db^2}$ is monotonically decreasing, we conclude that there exist a unique solution to $\phi(b) = 0$.

To prove the second statement, we take the derivative of p_t given by (26) to obtain

$$\dot{p}_t = -\sigma^2 \sin(\omega t + \theta).$$

If p_0, p_1 are the endpoints of p_t , then it is necessary that

$$|p_1 - p_0| = \left| \int_0^1 \dot{p}_t dt \right| \leq \int_0^1 |\dot{p}_t| dt \leq \sigma^2.$$

To show that there exist a path of the form (26) for any p_0, p_1 that satisfies $|p_1 - p_0| < \sigma^2$, we re-parameterize (26) as follows

$$p_t = c \cos(\omega t) + d \sin(\omega t),$$

with $(c^2 + d^2)\omega^2 = \sigma^4$. By setting p_t to p_0, p_1 at $t = 0, 1$, respectively, we obtain that

$$\begin{aligned} p_0 &= c, \\ p_1 &= c \cos(\omega) + d \sin(\omega). \end{aligned} \tag{29}$$

Therefore,

$$d = \frac{p_1 - p_0 \cos(\omega)}{\sin(\omega)}. \tag{30}$$

Next, substituting (29) and (30) to $\sin^2(\omega)(c^2 + d^2) = \sin^2(\omega)\frac{\sigma^4}{\omega^2}$ to obtain that

$$\frac{\sigma^4}{\omega^2} \sin^2(\omega) + 2p_0 p_1 \cos(\omega) = p_0^2 + p_1^2. \tag{31}$$

We denote the left hand side of the above equation by $\psi(\omega)$. Then, the following holds

$$\lim_{\omega \rightarrow 0} \psi(\omega) = \sigma^4 + 2p_0 p_1 \geq (p_1 - p_0)^2 + 2p_0 p_1 = p_0^2 + p_1^2.$$

Moreover, $\psi(\pi) = -2p_0 p_1 < 0$. Furthermore, it can be shown that

$$\frac{d\psi(\omega)}{d\omega} = \left(2\frac{\sigma^4}{\omega^3}(\omega \cos(\omega) - \sin(\omega)) - 2p_0 p_1 \right) \sin(\omega) < 0$$

for all $\omega \in (0, \pi)$. Therefore, there exists a unique solution to (31) for $\omega \in (0, \pi)$, which completes the proof. \square

IV. WEIGHTED-LEAST-SQUARES BASED COVARIANCE PATHS

For scalar-valued covariance, the Fisher-Rao metric $g_p(\dot{p})$ can be viewed as the squared norm $(\frac{\dot{p}}{p})^2$. For matrices, there is in general no unique ways to define matrix divisions. For example, in the following differential equation

$$\dot{P}_t = A_t P_t + P_t A_t', \quad (32)$$

the matrix A_t can be viewed as a non-commutative division of $\frac{1}{2}\dot{P}$ by P . For a given pair of matrices P_t and \dot{P}_t there are infinite A_t that satisfy (32). But there could be a unique one that minimizes or maximizes a quadratic function $f(A_t)$ whose optimal value provides a well-defined quadratic norm of the non-commutative division of \dot{P}_t by P_t . The optimal value of the quadratic function provides a way to define Riemmanian metrics on the manifold of covariance matrices in order to quantify the similarity between covariance matrices. This motivates our choice of the third objective function.

Specifically, for a matrix $A_t \in \mathbb{R}^{n \times n}$, we decompose it as $A_t = A_{t,s} + A_{t,a}$ where

$$A_{t,s} := \frac{1}{2}(A_t + A_t'),$$

$$A_{t,a} := \frac{1}{2}(A_t - A_t'),$$

are the symmetric and asymmetric parts of A_t , respectively. For a given scalar $\epsilon > 0$, we define the following weighted squared norm of A_t

$$\begin{aligned} f_\epsilon^{\text{wls}}(A_t) &:= \|A_{t,s}\|_F^2 + \epsilon \|A_{t,a}\|_F^2 \\ &= \frac{1+\epsilon}{2} \text{tr}(A_t A_t') + \frac{1-\epsilon}{2} \text{tr}(A_t A_t). \end{aligned}$$

Following (3), we consider the optimization problem in below:

$$\min_{P_t, A_t} \left\{ \int_0^1 \frac{1+\epsilon}{2} \text{tr}(A_t A_t') + \frac{1-\epsilon}{2} \text{tr}(A_t A_t) dt \mid \right. \\ \left. \dot{P}_t = A_t P_t + P_t A_t' + \sigma^2 I, P_0, P_1 \text{ specified} \right\}. \quad (33)$$

Proposition 4. *Given $P_0, P_1 \in \mathcal{S}_{++}^n$ and two scalars $\epsilon, \sigma > 0$. If there exists a pair of matrix-*

valued functions P_t, Π_t that satisfy

$$\dot{P}_t = -\frac{1+\epsilon}{2\epsilon}(\Pi_t P_t^2 + P_t^2 \Pi_t) + \frac{1-\epsilon}{\epsilon} P_t \Pi_t P_t + \sigma^2 I, \quad (34)$$

$$\dot{\Pi}_t = \frac{1+\epsilon}{2\epsilon}(\Pi_t^2 P_t + P_t \Pi_t^2) - \frac{1-\epsilon}{\epsilon} \Pi_t P_t \Pi_t, \quad (35)$$

with P_t being equal to P_0, P_1 at $t = 0, 1$, respectively, then P_t is a optimal solution to (33). Moreover, the optimal A_t is given by

$$A_t = -\frac{1}{2}(\Pi_t P_t + P_t \Pi_t) + \frac{1}{2\epsilon}(P_t \Pi_t - \Pi_t P_t). \quad (36)$$

Proof. Following the same method as in the proof of Proposition (2), we develop the necessary conditions for a stationary value using the following Hamiltonian

$$h_3(P_t, A_t, \Pi_t) = \text{tr} \left(\frac{1+\epsilon}{2} \text{tr}(A_t A_t') + \frac{1-\epsilon}{2} \text{tr}(A_t A_t) + \Pi_t (A_t P_t + P_t A_t' + \sigma^2 I) \right).$$

Setting $-\dot{\Pi}_t$ equal to partial derivative of $h_3(\cdot)$ with respect to P_t to obtain that

$$\dot{\Pi}_t = -\Pi_t A_t - A_t' \Pi_t. \quad (37)$$

Moreover, setting the partial derivative of $h_2(\cdot)$ with respect to A_t equal to zero to obtain that

$$(1+\epsilon)A_t + (1-\epsilon)A_t' + 2\Pi_t P_t = 0. \quad (38)$$

Thus, the symmetric and asymmetric part of A_t are equal to

$$A_{t,s} = -\frac{1}{2}(\Pi_t P_t + P_t \Pi_t),$$

$$A_{t,a} = \frac{1}{2\epsilon}(P_t \Pi_t - \Pi_t P_t).$$

Therefore (36) holds. Then, (34) and (35) can be obtained by substituting (36) into (2) and (37), respectively. \square

Moreover, the path defined by (34) and (35) also coincide with the path given by (18) and (19) for scalar-valued covariance. Therefore, the results from Proposition 3 can also be adapted to the solution of (33).

Proposition 5. *Given three positive scalars p_0, p_1 and σ . If $|p_1 - p_0| > \sigma^2$, then exists a unique solution to (33) which has the form of (25). If $|p_1 - p_0| < \sigma^2$, then there exists a unique solution to (33) which has the form of (26).*

Remark. *For any given $\epsilon \neq 0$ and a pair of initial values Π_0, P_0 , the pair of equations (34) and (35) provide a smooth path of covariance matrices. In the special case when $\epsilon = -1$, (34) and (35) is equivalent to the Fisher-Rao based path given by (18) and (19). In the noiseless situation, the existence and uniqueness of the covariance path that satisfy (34) and (35) has been shown in [1] for ϵ taking values around -1 .*

To understand the influence of input noise to the optimal covariance path, we consider a trajectory defined by (34) to (36) with given initial values P_0 and Π_0 and the symmetric and asymmetric parts of the system matrix A_t are initialized by (36). Then it is straightforward to verify that the asymmetric part of A_t given by (36) is constant, which is denoted by $A_{0,a}$ and is equal to $\frac{1}{2\epsilon}(P_0\Pi_0 - \Pi_0P_0)$. On the other hand, by taking the derivative of the symmetric part of A_t , denoted by $A_{t,s}$, we obtain that

$$\dot{A}_{t,s} = (1 + \epsilon)(A_{0,a}A_{t,s} + A_{t,s}A'_{0,a}) - \sigma^2\Pi_t. \quad (39)$$

Next, we apply change of variables to define

$$\hat{A}_t = e^{(1+\epsilon)A'_{0,a}t} (A_{t,s} + \epsilon A'_{0,a}) e^{(1+\epsilon)A_{0,a}t}.$$

Similarly, applying a time-varying change of coordinate to define

$$\begin{aligned} \hat{P}_t &= e^{(1+\epsilon)A'_{0,a}t} P_t e^{(1+\epsilon)A_{0,a}t}, \\ \hat{\Pi}_t &= e^{(1+\epsilon)A'_{0,a}t} \Pi_t e^{(1+\epsilon)A_{0,a}t}. \end{aligned}$$

Then the derivative of the new variable \hat{A}_t is equal to

$$\dot{\hat{A}}_t = -\sigma^2\hat{\Pi}_t. \quad (40)$$

Moreover, the derivative of \hat{P}_t is equal to

$$\begin{aligned}\dot{\hat{P}}_t &= (1 + \epsilon)A'_{0,a}t\hat{P}_t + (1 + \epsilon)\hat{P}_tA_{0,a} \\ &\quad + e^{(1+\epsilon)A'_{0,a}t}(A_tP_t + P_tA'_t + \sigma^2I)e^{(1+\epsilon)A_{0,a}t} \\ &= \hat{A}_t\hat{P}_t + \hat{P}_t\hat{A}'_t + \sigma^2I.\end{aligned}\tag{41}$$

Similarly, the derivative of $\hat{\Pi}_t$ is given by

$$\dot{\hat{\Pi}}_t = -\hat{A}'_t\hat{\Pi}_t - \hat{\Pi}_t\hat{A}_t.\tag{42}$$

Combining (40) and (42), we obtain that the covariance path is determined by the following second-order differential equation in the rotating frame

$$\ddot{\hat{A}}_t + \hat{A}'_t\dot{\hat{A}}_t + \dot{\hat{A}}'_t\hat{A}_t = 0,\tag{43}$$

with the initial values given by

$$\hat{A}_0 = A_{0,s} + \epsilon A'_{0,a} = -P_0\Pi_0,\tag{44}$$

$$\dot{\hat{A}}_0 = -\sigma^2\Pi_0.\tag{45}$$

The special case when $\sigma = 0$, the matrix \hat{A}_t is clearly constant based on (40). Therefore, (41) becomes a linear time-invariant system whose solution is given by the standard expression $\hat{P}_t = e^{\hat{A}_0 t}P_0e^{\hat{A}'_0 t}$. Then, transforming \hat{A}_t and \hat{P}_t to the original coordinate to obtain that

$$A_t = e^{(1+\epsilon)A_{0,a}t}A_0e^{(1+\epsilon)A'_{0,a}t},\tag{46}$$

$$P_t = T_{\epsilon,t}(A)P_0T_{\epsilon,t}(A)',\tag{47}$$

where $T_{\epsilon,t}(A) = e^{(1+\epsilon)A_{0,a}t}e^{(A_{0,s} + \epsilon A'_{0,a})t}$, $A_{0,s} = -\frac{1}{2}(\Pi_0P_0 + P_0\Pi_0)$, $A_{0,a} = \frac{1}{2\epsilon}(P_0\Pi_0 - \Pi_0P_0)$. $T_{\epsilon,t}(A)$ is the state transition matrix which satisfies that $\dot{T}_{\epsilon,t}(A) = A_tT_{\epsilon,t}(A)$. It is interesting to note that the system matrix A_t has a rotating eigenspace. If ϵ is sufficiently close to -1 , then there exists a unique covariance path of the form (45) that connects any given $P_0, P_1 \in \mathbb{S}_{++}^n$ [1].

V. EXAMPLE

A. Comparing scalar-valued covariance paths

In this example, we compare scalar-valued covariance paths given by the closed-form expressions in (6) and (25) to (26). Figure 1 illustrates several covariance paths with the initial value being $P_0 = 6$ and $\sigma = 4$. These plots clearly illustrate the differences between the paths obtained from OMT and the Fisher-Rao metric, especially between the paths whose endpoints at $t = 1$ are far away from $P_0 + \sigma^2$, which is equal to 22 in this example.

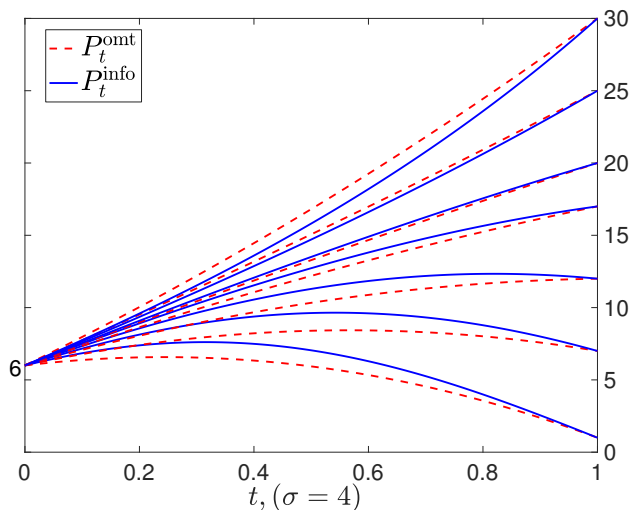


Fig. 1: An illustration of the covariance paths. The dashed red lines denoted by P_t^{omt} illustrate the paths given by (6) based on OMT. The solid blue lines denoted by P_t^{info} illustrate the covariance paths given by (25) to (26) based on the Fisher-Rao metric.

B. Comparing matrix-valued covariance paths

In this example, we illustrate the difference between the above covariance paths using two fixed endpoints given by

$$P_0 = \begin{bmatrix} 1 & 0 \\ 0 & 0.3 \end{bmatrix}, P_1 = \begin{bmatrix} 0.3 & 0 \\ 0 & 1 \end{bmatrix}. \quad (48)$$

Fig. 2a shows the OMT-based paths in (6) using several different values for σ , where the ellipsoids denote isocontour of the quadratic function $\mathbf{x}'P_t\mathbf{x} = r^2$ with $r = 0.5$. Fig. 2b illustrates the Fisher-Rao-based paths given by the (21). Since P_0 and P_1 commute, the paths are obtained by using the closed-form expressions in (25) to (26) to the diagonal entries. Though there are minor

differences between the two sets of covariance paths, all the P_t 's along the two paths have the same eigenspace.

Regarding the covariance paths defined by (34) and (35), their closed-form solutions are currently unknown. For this particular pair of end points, there exists multiple local optimal paths. Specifically, we consider the solution to (33) when $\epsilon = 0$. In this case, any asymmetric system matrix A of the form

$$A = \begin{bmatrix} 0 & \pm \frac{(2k+1)\pi}{2} \\ \mp \frac{(2k+1)\pi}{2} & 0 \end{bmatrix}, \quad (49)$$

is an optimal solution because the corresponding objective value is equal to zero. The corresponding covariance paths are of the form

$$P_{\pm,t} = \begin{bmatrix} 0.3 + 0.7 \cos^2\left(\frac{(2k+1)\pi}{2}t\right) & \pm 0.7 \cos\left(\frac{(2k+1)\pi}{2}t\right) \sin\left(\frac{(2k+1)\pi}{2}t\right) \\ \pm 0.7 \cos\left(\frac{(2k+1)\pi}{2}t\right) \sin\left(\frac{(2k+1)\pi}{2}t\right) & 0.3 + 0.7 \sin^2\left(\frac{(2k+1)\pi}{2}t\right) \end{bmatrix} + \sigma^2 It.$$

In order to obtain a numerical solution for the covariance paths given by (34) and (35) with $\epsilon > 0$, we apply the *lsqnonlin* nonlinear optimization toolbox and the *ode45* functions in MATLAB (The MathWorks, Inc., Natic, MA) to solve for Π_0 so that a path P_t starts from P_0 will have the least square error relative to P_1 at $t = 1$. We first set $\epsilon = 0.001$ and choose two different initial values for $\hat{\Pi}_0$ used in the optimization algorithms given by

$$\hat{\Pi}_{\pm,0} = \pm \frac{1}{700} \begin{bmatrix} 0 & \pi \\ \pi & 0 \end{bmatrix},$$

so that the corresponding system matrices given by (36) approximately satisfy (49). Next, we gradually increase ϵ using a step size of 0.001 and use the optimal Π_0 from the previous step as the initial value. The left and right panels of Fig. 3 illustrate two branches of locally optimal paths corresponding to the two different initial values of Π_0 with $\sigma = 0.5$ and several different values for ϵ . All the numerical solutions satisfy the endpoints with the Frobenius norm of the residuals at the order of 10^{-6} or smaller. Very different from the paths shown in (2), the paths in Fig. 3 have rotating eigenspace where the rotation direction depends on the initial choice of Π_0 . Moreover, as ϵ increase, the paths become similar to those shown in Fig. 2.

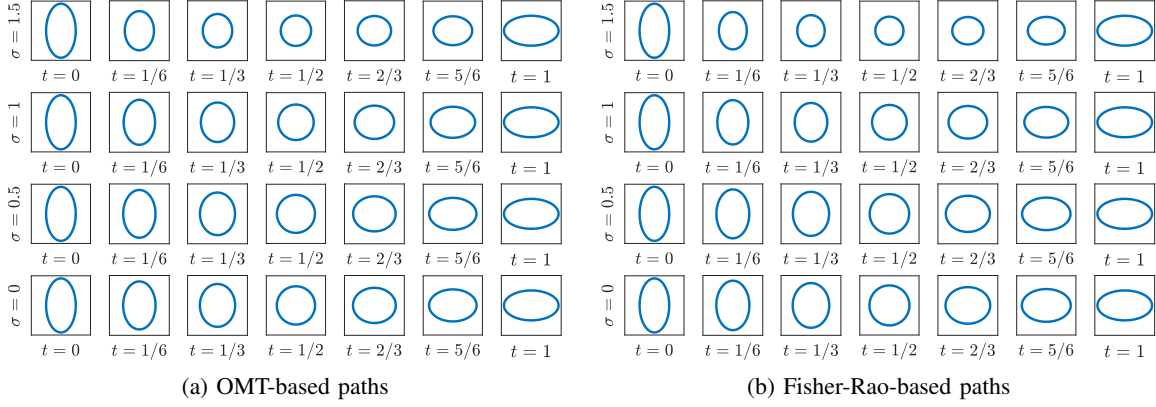


Fig. 2: An illustration of the covariance paths obtained using (6) (Left) and (21) (Right), respectively, with the two endpoints given by P_0 and P_1 in (48).

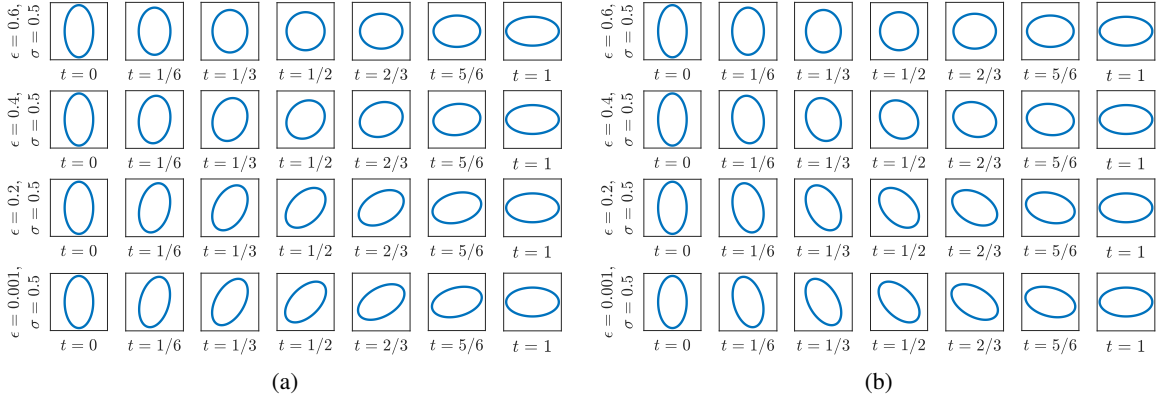


Fig. 3: An illustration of two branches, i.e. (a) and (b), of locally-optimal covariance paths obtained using (34) and (35) with different initial values for Π .

C. Fitting noisy measurements of functional MRI data

In this example, we apply the proposed covariance paths to fit noisy sample covariance matrices of a stochastic process based on a resting-state functional MRI (rsfMRI) dataset used in [1]. The interested reader is referred to [1] for more detailed information on the data. This problem is formulated as follows. Given K sample covariance matrices, $\tilde{P}_{t_1}, \dots, \tilde{P}_{t_K}$ based on K segments of a multivariate time series, find a smooth covariance path P_t that minimizes

$$\min_{P_t} \sum_{k=1}^K \|P_{t_k} - \tilde{P}_{t_k}\|_{\mathbb{F}}^2. \quad (50)$$

In this example, we have $K = 10$ noisy sample covariance from a 7-dimensional process. We apply three parametric models of covariance path to fit these measurements using the *fminsdp* function in MATLAB. The first one is the closed-form expression given by (6) which is parameterized by P_0, Π_0 and σ . The optimal solution is denoted by \hat{P}_t^{omt} . The second model is based on the differential equation (18) and (19) which is implemented by the *ode45* function in MATLAB. The estimated path is denoted by \hat{P}_t^{info} . Note again that this model is a special case of (34) and (35) when $\epsilon = -1$. The more general model in (34) and (35) relies on the estimation of an additional parameter ϵ . Since the differential equations are highly nonlinear in terms of ϵ , we find that the MATLAB algorithm only provides a local optimal value of ϵ depending on its initial value. In order to obtain a reliable covariance path to understand the rotation of energy among the variables, we apply the rotating-system based covariance path in (46) to fit the measurements by setting $\epsilon = 20$ as used in [1]. The estimated path is denoted by \hat{P}_t^{wls} .

The discrete markers in Fig. 4 illustrate the noisy sample covariance of 6 entries of the covariance matrices. The blue, green and red plots are the estimated paths given by \hat{P}_t^{omt} , \hat{P}_t^{info} , and \hat{P}_t^{wls} , respectively. The normalized squared errors corresponding to the three paths are equal to 0.1842, 0.1696 and 0.1506, respectively. The much lower estimation error corresponding to \hat{P}_t^{wls} is because of its capability in tracking rotations in the covariance.

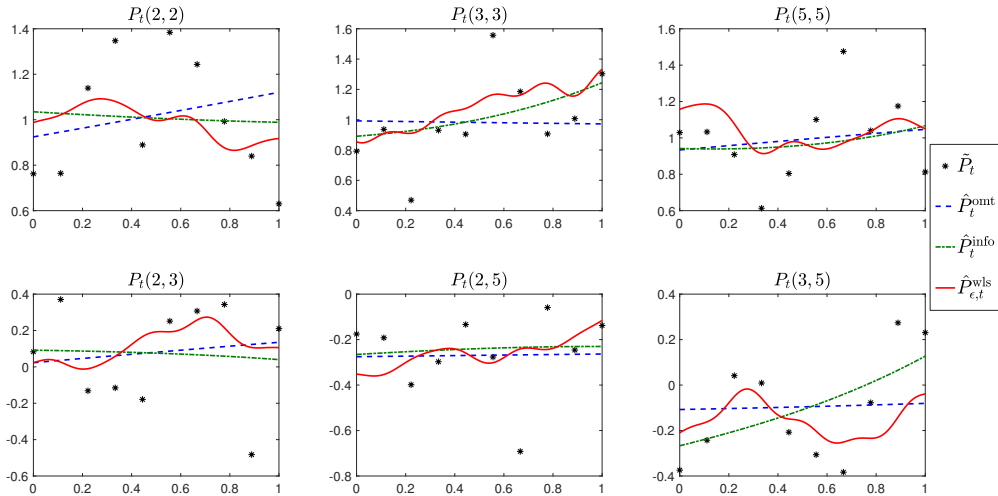


Fig. 4: These plots illustrate the noisy sample covariance \tilde{P}_t and the fitting results of three covariance paths based on a rsfMRI dataset.

VI. DISCUSSION AND CONCLUSION

In this paper, we have investigated three types of covariance paths by using different regularizations on linear stochastic systems. The first covariance path is given by the solution to the Schrödinger bridge problem for multivariate Gaussian and optimal mass transport. The second type of covariance path is based on a generalization of the Fisher-Rao metric with a stochastic input term. The third type of covariance paths is obtained using a weighted-least-square regularizations on the system matrices. It is interesting to remark that the Fisher-Rao metric can be viewed as a weight-mass-transport cost. The corresponding covariance path is a special case of the weighted-least-square based solutions. The main contributions of this work include the differential-equation formulations for the last two types of covariance paths and the closed-form expressions for the scalar-valued case.

The general theme of this paper is closely related to the work in [12], [18]–[22] which all focused on investigating smooth paths connecting positive definite matrices. The proposed approach is based on different regularizations functions of system matrices which distinguishes this paper from early work. Finally, we remark that a main motivation of this paper is from a neuroimaging application on analyzing functional brain networks using resting-state functional MRI data. The proposed covariance paths with rotating eigenspace may provide a useful tool to understand the oscillations and directed connections among brain networks, which will be further explored in our future work.

APPENDIX

REFERENCES

- [1] L. Ning, “Regularization of covariance matrices on Riemannian manifolds using linear systems,” *under review*, 2018.
- [2] C. Villani, *Topics in Optimal Transportation*. Amer. Math. Soc., 2003.
- [3] S. Rachev and L. Rüschendorf, *Mass transportation problems. Vol. I and II. Probability and its Applications*. Springer, New York, 1998.
- [4] M. Knott and C. S. Smith, “On the optimal mapping of distributions,” *Journal of Optimization Theory and Applications*, vol. 43, no. 1, pp. 39–49, May 1984.
- [5] A. Takatsu, “On Wasserstein geometry of the space of Gaussian measures,” *ArXiv e-prints*, Jan. 2008.
- [6] E. Schrödinger, “Über die Umkehrung der Naturgesetze,” *Sitzungsberichte Preuss. Akad. Wiss. Berlin. Phys. Math.*, pp. 144–153, 1931.
- [7] C. Léonard, “A survey of the Schrödinger problem and some of its connections with optimal transport,” *ArXiv e-prints*, Aug. 2013.
- [8] Y. Chen, T. T. Georgiou, and M. Pavon, “On the relation between optimal transport and Schrödinger bridges: A stochastic control viewpoint,” *Journal of Optimization Theory and Applications*, vol. 169, no. 2, pp. 671–691, May 2016.

- [9] C. Rao, "Information and the accuracy attainable in the estimation of statistical parameters," *Bull. Calcutta Math. Soc.*, vol. 37, pp. 81 – 91, 1945.
- [10] S.-I. Amari and H. Nagaoka, *Methods of information geometry*. Amer. Math. Soc., 2000.
- [11] A. Uhlmann, "The metric of bures and the geometric phase," in *Quantum Groups and Related Topics: Proceedings of the First Max Born Symposium*, R. Gielerak, J. Lukierski, and Z. Popowicz, Eds., 1992, p. 267.
- [12] L. Ning, X. Jiang, and T. Georgiou, "On the geometry of covariance matrices," *IEEE Signal Processing Letters*, vol. 20, no. 8, pp. 787–790, Aug 2013.
- [13] R. Bhatia, T. Jain, and Y. Lim, "On the Bures-Wasserstein distance between positive definite matrices," *ArXiv e-prints*, Dec. 2017.
- [14] Y. Chen, T. T. Georgiou, and M. Pavon, "Optimal steering of a linear stochastic system to a final probability distribution, part I," *IEEE Transactions on Automatic Control*, vol. 61, no. 5, pp. 1158–1169, May 2016.
- [15] —, "Optimal steering of a linear stochastic system to a final probability distribution, part II," *IEEE Transactions on Automatic Control*, vol. 61, no. 5, pp. 1170–1180, May 2016.
- [16] M. Moakher, "Means and averaging in the groups of rotations," *SIAM J. Matrix Anal. Appl.*, vol. 24, no. 1, pp. 1–16, 2002.
- [17] C. Lenglet, M. Rousson, R. Deriche, and O. Faugeras, "Statistics on the manifold of multivariate normal distributions: Theory and application to diffusion tensor MRI processing," *Journal of Mathematical Imaging and Vision*, vol. 25, no. 3, pp. 423–444, Oct 2006.
- [18] X. Jiang, L. Ning, and T. T. Georgiou, "Distances and riemannian metrics for multivariate spectral densities," *IEEE Transactions on Automatic Control*, vol. 57, no. 7, pp. 1723–1735, July 2012.
- [19] L. Ning, T. T. Georgiou, and A. Tannenbaum, "On matrix-valued monge-kantorovich optimal mass transport," *IEEE Transactions on Automatic Control*, vol. 60, no. 2, pp. 373–382, 2015.
- [20] Y. Chen, T. Georgiou, and A. Tannenbaum, "Matrix Optimal Mass Transport: A Quantum Mechanical Approach," *ArXiv e-prints*, Oct. 2016.
- [21] Y. Chen, T. T. Georgiou, L. Ning, and A. Tannenbaum, "Matricial wasserstein-1 distance," *IEEE Control Systems Letters*, vol. 1, no. 1, pp. 14–19, July 2017.
- [22] K. Yamamoto, Y. Chen, L. Ning, T. T. Georgiou, and A. Tannenbaum, "Regularization and interpolation of positive matrices," *IEEE Transactions on Automatic Control*, vol. PP, no. 99, pp. 1–1, 2017.